A ribulose-1,5-bisphosphate carboxylase/oxygenase (RubisCO)-like protein from *Chlorobium tepidum* that is involved with sulfur metabolism and the response to oxidative stress

Thomas E. Hanson and F. Robert Tabita*

Department of Microbiology and Plant Molecular Biology/Biotechnology Program, Ohio State University, 484 West 12th Avenue, Columbus, OH 43210-1292

A gene encoding a product with substantial similarity to ribulose-1,5-bisphosphate carboxylase/oxygenase (RubisCO) was identified in the preliminary genome sequence of the green sulfur bacterium *Chlorobium tepidum*. A highly similar gene was subsequently isolated and sequenced from *Chlorobium limicola* f.sp. *thiosulfatophilum* strain Tassajara. Analysis of these amino acid sequences indicated that they lacked several conserved RubisCO active site residues. The *Chlorobium* RubisCO-like proteins are most closely related to deduced sequences in *Bacillus subtilis* and *Archaeoglobus fulgidus*, which also lack some typical RubisCO active site residues. When the *C. tepidum* gene encoding the RubisCO-like protein was disrupted, the resulting mutant strain displayed a pleiotropic phenotype with defects in photopigment content, photoautotrophic growth and carbon fixation rates, and sulfur metabolism. Most important, the mutant strain showed substantially enhanced accumulation of two oxidative stress proteins. These results indicated that the *C. tepidum* RubisCO-like protein might be involved in oxidative stress responses and/or sulfur metabolism. This protein might be an evolutionary link to *bona fide* RubisCO and could serve as an important tool to analyze how the RubisCO active site developed.

Ribulose 1,5-bisphosphate carboxylase/oxygenase [EC 4.1.1.39 (RubisCO)] occupies a central position in the global carbon cycle and is one of two key and unique catalysts of the Calvin–Benson–Bassham cycle that enable inorganic atmospheric carbon dioxide (CO_2) to be converted into organic cellular constituents. The other key and unique Calvin–Benson–Bassham cycle catalyst is phosphoribulokinase (EC 2.7.1.19), which catalyzes the phosphorylation of ribulose 5-phosphate to form ribulose 1,5-bisphosphate (RuBP), the substrate for RubisCO. Genes encoding functional RubisCO proteins are present in bacteria, archaea, and eukaryotes, and several of these have been subjected to intense biochemical, biophysical, and genetic studies (1, 2). One question these studies have not elucidated is where, evolutionarily speaking, did RubisCO come from?

Green sulfur bacteria are photoautotrophic organisms that use the reductive tricarboxylic acid cycle for CO_2 fixation (3–5). The reductive tricarboxylic acid cycle, in contrast to the Calvin–Benson–Bassham cycle, utilizes soluble ferredoxin-linked oxidoreductases to reverse the decarboxylation reactions catalyzed by membrane-bound dehydrogenases of the oxidative tricarboxylic acid pathway and fix CO_2 into cellular constituents (5). Reduced sulfur compounds (sulfide, thiosulfate, elemental sulfur) are oxidized to provide the reducing equivalents for CO_2 fixation (4) with electrons donated ultimately to ferredoxin. Reduced ferredoxin drives the synthesis of pyruvate and α-ketoglutarate by the reductive carboxylation of acetyl-CoA and succinyl-CoA, respectively (5). *Chlorobium tepidum* is a moderately thermophilic, genetically amenable green sulfur bacterium whose 2.1-Mb genome has been completely sequenced at The Institute for Genomics Research (TIGR). After a search of the publicly available *C. tepidum* genomic sequence database, a gene encoding a RubisCO-like protein (RLP) was identified. The presence of RubisCO in green sulfur bacteria has historically been controversial (3, 6–12); in this study, a nearly identical RLP gene was also isolated from *Chlorobium limicola*, the organism originally studied (3, 6–12). Both gene products were shown to be members of a phylogenetic cluster of archaeal and bacterial RLP sequences that lack a complete RubisCO active site.

Gene disruption experiments indicated that the *C. tepidum* RLP was not essential for growth. Phenotypic analysis of the RLP mutant strain indicated a role for this gene product primarily in sulfur metabolism and oxidative stress responses. These phenotypic studies along with studies of purified recombinant *C. tepidum* RLP do not support a direct role for this gene product in carbon fixation. On the basis of these results, we suggest that this protein has hallmarks expected of a prospective evolutionary precursor of *bona fide* RubisCO. RubisCO belongs to a structurally similar class of proteins called α/β barrel enzymes (13–15). Such proteins have been shown to be good targets for *in vitro*-directed enzyme evolution, with the α/β barrel scaffold thought to provide evolutionary flexibility (16). The present study may be considered the first stage toward implicating a common evolutionary origin of the RLP molecules with *bona fide* RubisCO, providing a natural example of the development of functionally different proteins with similar structural motifs.

Materials and Methods

Strains and Growth Conditions. *Chlorobium* strains were grown in PF-7 medium buffered to pH 6.95 with 10 mM Mops, as described (17–20). *C. tepidum* strain WT2321 and derivatives were grown at 42°C for antibiotic selection, but at the optimum of 47°C for physiological measurements (19, 20). *C. limicola* was grown at room temperature. The protein content of *Chlorobium* cultures was used to monitor growth. Extracts were prepared and protein concentration measured by a dye-binding assay, as described (17).

Escherichia coli strain JM109 was used for cloning, whereas *E.*

BIOCHEMISTRY

coli BL21(DE3) was used for the production of recombinant *C. tepidum* RLP. *E. coli* was routinely grown in Luria–Bertani (LB) broth or on LB plates (21). Antibiotics used for plasmid selection in *E. coli* were: ampicillin, 100 μg ml^{-1}; kanamycin 50 μg ml^{-1}; streptomycin (Sm) 25 μg ml^{-1}; and spectinomycin (Sp) 25 μg ml^{-1}. Antibiotics and media components were purchased from Sigma or Fisher.

Transformation and Mutant Selection. Strain Ω::RLP, a derivative of WT2321 containing an Ω cassette-disrupted RLP gene (22), was constructed by using linear DNA transformation as described by Chung *et al.* (23) with the exception that a two-step selection procedure was used. For the initial selection, dilutions of transformation mixes were plated on photoheterotrophic chlorobium plating (CP) medium plates (19) containing 15 μg ml^{-1} Sp + 15 μg ml^{-1} Sm (15 μg ml^{-1} Sp + Sm). After 5 days of growth, colonies were picked and restreaked onto photoheterotrophic CP medium containing 100 μg ml^{-1} Sp + Sm. After 7 days of growth, DNA was prepared from cells on plates (24), and the genotype of strains was determined by Southern blotting.

Strain Ω::SDR, a derivative of WT2321 containing a disrupted short-chain dehydrogenase/reductase homolog gene, was constructed by linear DNA transformation by using a single-step selection. Dilutions of transformation mixes resuspended from nonselective plates were plated on photoheterotrophic CP medium containing 200 μg ml^{-1} Sp + Sm. Isolated colonies obtained after 4 days of growth were restreaked onto the same medium and grown for DNA preparation and Southern analysis. Spontaneous Sp + Sm resistance, e.g., colonies growing in the absence of exogenous DNA, was not observed above 25 μg ml^{-1} Sp + Sm. Spontaneously arising Sp + Sm resistant strains could not be grown above 25 μg ml^{-1} Sp + Sm (data not shown).

Molecular Biology Protocols. Genomic DNA purification, Southern blotting, and PCR were carried out by standard protocols (17, 21). The *C. tepidum* RLP ORF was PCR amplified with primers rbc-*Nde*I-F 5′-ACCGGATCAA*CATATG*AATGCT-GAAG-3′ and rbc-*Bam*HI-R 5′-GCAGC*GGATCC*TT-TCAGTCCTGCTTC-3′. The *C. limicola* RubisCO-like ORF was PCR amplified with primer rbc-*Nde*I-F and a new primer, rbc-*Eco*RV-R 5′-GCGCCGCGTT*GATATC*CTGCTTCTTC-3′. Restriction sites indicated in the primer names are underlined in the sequences. PCR products were cloned by using the pCR-Script Amp SK(+) kit (Stratagene). DNA sequences were determined with a dye-terminator cycle DNA sequencing kit (Thermosequenase II, Amersham Pharmacia Biotech) by using an ABI 310 Genetic Analyzer (Perkin–Elmer, Applied Biosystems Division).

Antibody Preparation and Immunoblotting. SDS/PAGE purified (21) recombinant *C. tepidum* RLP was used to produce rabbit polyclonal antibodies (Cocalico Biologicals). Serum obtained after two boosts was used at a dilution of 1:3,000 for immunoblotting of SDS/PAGE gels transferred to poly(vinylidene difluoride) membranes (Millipore). Immunodetection was performed as described (25).

Elemental Sulfur Quantitation. Chemical analysis for elemental sulfur was performed by sequential methanol and *n*-hexane extractions as described by Brune (4). Elemental sulfur in *n*-hexane was quantitated by its absorbance at 260 nm (ε, 25.4 g^{-1} liter cm^{-1}) (4). Methanol (HPLC grade) and *n*-hexane were purchased from Fisher.

Preparation of Proteins for N-Terminal Sequencing. Cell extract from strain Ω::RLP (800 μg protein) was loaded onto two preparative SDS/PAGE gels. After electrophoresis and brief staining, the hyperexpressed band was excised with a razor blade. Proteins were isolated from the gel slice (21), loaded onto a second SDS/PAGE gel, and then transferred to a high-density Sequi-Blot poly(vinylidene difluoride) membrane (Bio-Rad). The membrane was briefly stained, and the 25-kDa band of interest was excised. N-terminal sequence was determined with an ABI 477 automated sequencer (Perkin–Elmer Applied Biosystems) at the University of California, Davis, Protein Structure Laboratory.

Biochemical Activity Assays. Superoxide dismutase activity was measured by its interference with xanthine oxidase-dependent cytochrome *c* reduction (26). *O*-acetylserine sulfhydrylase activity was measured as described (27). Whole cell CO_2 fixation rates were measured in midlogarithmic phase cultures by amending cultures with H$^{14}CO_3^-$ and stopping at time points with propionic acid. Cells were collected on glass fiber filters and washed with propionic acid. Filters were counted by liquid scintillation, rates determined from linear regression analysis of plots of ^{14}C incorporation vs. time, and then normalized to the protein content of the culture sample. Substrates and reagents were purchased from Sigma.

Results

Green Sulfur Bacteria Contain a Gene Encoding a RLP. BLASTX searches (28) of the preliminary *C. tepidum* genomic sequence were carried out at The Institute for Genomics Research (TIGR) (www.tigr.org) or the National Center for Biotechnology Information (www.ncbi.nlm.nih.gov) web sites with representative form I and II RubisCO amino acid sequences. A single homologous ORF was detected. PCR primers were designed and used to amplify the ORF from *C. tepidum* genomic DNA. This PCR product was labeled as a probe in Southern hybridizations against *C. tepidum* and *C. limicola* genomic DNA, detecting a single hybridizing band in each organism. PCR primers designed for the *C. tepidum* gene were used to amplify the RubisCO-like gene from *C. limicola*. Both PCR products were cloned in pCR-Script Amp SK(+) generating pCTENB-1 (*C. tepidum*) and pCLENE-1 (*C. limicola*). Two independent clones of each were completely sequenced on both strands. The *C. tepidum* sequence was found to be in complete agreement with that determined by TIGR (data not shown).

The PCR products from *C. tepidum* and *C. limicola* contained an ORF that was 95.2% identical at the amino acid level and 89.3% identical at the nucleotide level. The predicted amino acid sequences for the *C. tepidum* and *C. limicola* ORFs were used in multiple sequence alignments to generate a phylogenetic tree (Fig. 1). The *C. tepidum* and *C. limicola* predicted amino acid sequences are members of a branch within the RubisCO family, labeled form IV, distinct from the form I, II, and III subfamilies. The other members of this subfamily are the *Bacillus subtilis ykrW* and *Archaeoglobus fulgidus rbcL*-1 gene products. No distinct physiological role has been proposed for any member of this family. The *B. subtilis ykrW* gene is a member of the S box regulon that responds to the availability of methionine (29). S box motifs can be detected in the *C. tepidum* genomic sequence, but no S box sequence is apparent in the upstream region of the gene encoding the RLP (data not shown).

A unifying characteristic of the form IV subfamily is the lack of multiple conserved active site residues found in forms I–III RubisCOs (Fig. 2). Both *Chlorobium* RubisCO-like sequences lack 9 of 19 active site residues. *B. subtilis ykrW* lacks 6 and *A. fulgidus rbcL*-1 lacks 3 of 19 key active site residues. Consistent with this observation, none of the form IV enzymes have been demonstrated to have robust RubisCO activity (J.-P. Yu, M. W. Finn, and F.R.T., unpublished work), whereas members of forms I–III have been shown to possess *bona fide* RubisCO activity. It is for this reason that we refer to the form IV subfamily as RLPs.

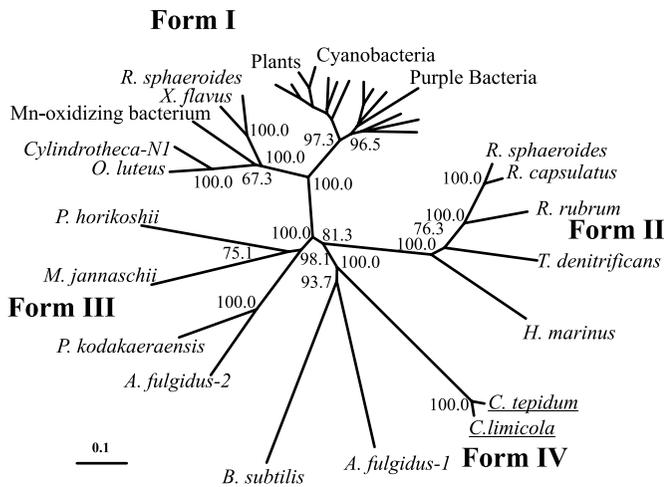The *Chlorobium* RLPs are specifically altered at sites involved

Form I

Fig. 1. Phylogenetic tree of RubisCO (Forms I–III) and RubisCO-like amino acid sequences (Form IV) from various organisms. Multiple sequence alignments and trees were produced with CLUSTAL X and visualized with TREE VIEW 1.4. Bootstrap values indicated at the nodes are the percentage of times that particular node appeared in 1,000 trials.

in binding both phosphate groups of RuBP, sites involved in binding and stabilizing the transition state, and lysine 174, which in turn controls the pKa of lysine 172 that accepts a proton

Fig. 2. Partial amino acid sequence alignment of form I RubisCO (*Synechococcus* sp. strain PCC 6301; I-*Syn* 6301), form II RubisCO (*Rhodospirillum rubrum*; II-*Rr*), form III RubisCO (*Methanococcus jannaschii*; III-*Mj*) and form IV RLPs from *Archaeoglobus fulgidus* (IV-*Af*-RbcL-1), *Bacillus subtilis* (IV-*Bs*-YkrW), *C. tepidum* (IV-*Ct*-RLP) and *C. limicola* (IV-*Cl*-RLP). Active site residues are highlighted in black. Residues deviating from the active site consensus are highlighted in gray. C, residues involved in catalysis; R, residues involved in RuBP binding. The alignment is numbered according to the *Synechococcus* sp. strain PCC 6301 sequence.
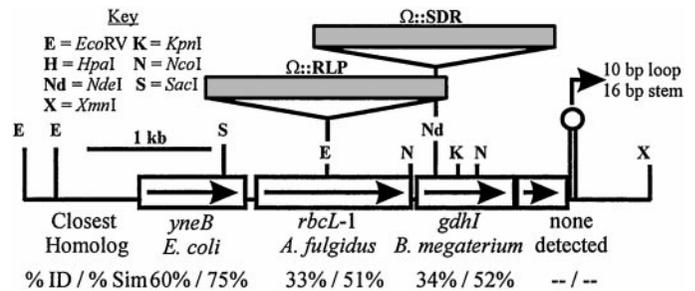

Fig. 3. Physical map of the *C. tepidum* genome surrounding the gene encoding the RLP and strategy for mutant construction. The closest homolog for each ORF was identified by BLASTP searches of the nonredundant protein database at the National Center for Biotechnology Information. Percent identity and similarity are at the amino acid level. The positions of the Ω cassette insertions are designated by the name of the resulting mutant strain.

during the catalytic cycle (2). Interestingly, two residues involved in binding the phosphate at C-1 and oxygen at C-4 of RuBP (glycine 380 and serine 378, respectively) are switched in the *Chlorobium* RLPs. The net effect of these alterations would be expected to greatly compromise the catalytic proficiency of RubisCO. Active site residues that are present in the *Chlorobium* RLPs are those involved in important catalytic events; e.g., the lysine that is carbamylated during activation of RubisCO and the entire signature motif—GKDFXKXDE—surrounding this lysine, which is involved in divalent cation binding and catalysis. All RLPs share a conservative substitution of isoleucine or leucine for phenylalanine at position 196 in the RubisCO motif. Molecular modeling of either the wild-type *C. tepidum* sequence or the *C. tepidum* sequence altered to contain all of the RubisCO active site residues in their correct positions did not produce meaningful results (data not shown).

RuBP-Dependent CO₂ Fixation in *C. tepidum*. Recombinant *C. tepidum* RLP synthesized in *E. coli* was soluble and could be easily purified, but it did not possess any detectable RuBP-dependent carboxylase or oxygenase activity (data not shown). Western blots using antiserum raised against the purified recombinant *C. tepidum* RLP indicated that the protein was synthesized constitutively in strain WT2321 (data not shown). A very low level of RuBP-dependent CO_2 fixation, 0.7 nmol CO_2 fixed min^{-1} (mg protein)$^{-1}$, could be detected in crude extracts of *C. tepidum* WT2321, but this activity was not abolished by the addition of 100 μM carboxyarabinitol bisphosphate (CABP), a tight binding transition state analog inhibitor (30). This result suggested that the observed RuBP-dependent CO_2 assimilation was not because of typical RubisCO activity. Control experiments with the form III RubisCO from *Methanococcus jannaschii* (31) demonstrated complete inhibition of RubisCO activity with 100 μM CABP (data not shown).

Construction of a *C. tepidum* Mutant Strain Lacking the RLP. The gene encoding the *C. tepidum* RLP is located in a group of four ORFs that could potentially be cotranscribed (Fig. 3). An ORF encoding a homolog of the *E. coli yneB* gene terminates 99-bp upstream of the initiation codon for the *C. tepidum* RLP ORF. The function of *yneB* is not known. Two ORFs are located downstream of the *C. tepidum* RLP ORF. The ORF immediately downstream initiates 38 bp after the RLP termination codon and encodes a predicted 32.5-kDa homolog of *gdhI* from *Bacillus megaterium* (32). The *gdhI* gene product is a developmentally regulated glucose dehydrogenase that belongs to the short chain dehydrogenase/reductase superfamily of protein sequences (33). The furthest downstream ORF initiates 11 bp after the termination codon of the *gdhI* homolog. No significant homologs

Hanson and Tabita

Table 1. Growth and whole cell CO$_2$ fixation rates of WT2321, strain Ω::RLP and strain Ω::SDR

Strain	Doubling time* growth condition			Whole cell CO$_2$ fixation[†] growth condition	
	CO$_2$	CO$_2$ + acetate	CO$_2$ + Cys	CO$_2$	CO$_2$ + acetate + pyruvate
WT2321	2.0 ± 0.3	1.9 ± 0.3	ND[‡]	1,719	514
Ω::RLP	7.7 ± 2.0	2.9 ± 0.6	2.7 ± 0.4	599	319
Ω::SDR	1.9 ± 0.3	ND	ND	ND	ND

*Doubling time in hours. Data are the mean ± standard deviation from three to five independent cultures for each condition. Starter cultures were from the same growth condition and were in mid- to late-logarithm phase (12–16 h old, <100 μg protein ml^{-1}). Cultures were inoculated to a density of 2–4 μg protein ml^{-1}.
[†]nmol CO$_2$ assimilated (min·mg protein)$^{-1}$. Data is the average of two independent log phase cultures.
[‡]ND, not determined.

to the predicted 18.5-kDa amino acid sequence of this ORF were found in database searches. Downstream of the putative operon is a stem–loop structure consisting of a 16-bp stem and 10-bp loop. Similar structures are found downstream of other operons and ORFs in green sulfur bacteria (34–36).

Two mutant strains of *C. tepidum* were constructed by linear transformation, a known means of genetic transfer in the *Chlorobiaceae* (23). The facile protocols described here should be applicable to all desired gene disruptions in *C. tepidum*. Strain Ω::RLP carried the Ω cassette integrated into the chromosome at an *Eco*RV site midway through the gene encoding the RLP (Fig. 3). Strain Ω::SDR carried the Ω cassette integrated into an *Nde*I site in the 5′ one-third of the *gdhI*-short chain dehydrogenase/reductase homolog (Fig. 3). Strain Ω::SDR thus served as a control for polar effects on downstream ORFs arising from the insertion carried by strain Ω::RLP. Neither gene product appeared to be essential for growth of *C. tepidum*. Extracts of Ω::RLP strains lacked the RLP, and Ω::SDR strains contained the same level of RLP as strain WT2321 (data not shown). Thus, the insertion of the Ω cassette into the gene encoding the *C. tepidum* RLP completely abolished its synthesis, and presumably its function, whereas an insertion downstream did not affect RLP levels.

Loss of the *C. tepidum* RLP Causes a Pleiotropic Phenotype. Analysis of the mutant strains identified several distinct phenotypes specifically associated with the loss of the RLP protein in strain Ω::RLP. An obvious difference was that cultures of strain Ω::RLP were a lighter shade of green than cultures of strain Ω::SDR or WT2321 at similar biomass densities. Strain Ω::RLP contained 20% less of the antenna photopigment bacteriochlorophyll *c* (BChl *c*) (20) than either parental strain WT2321 or strain Ω::SDR, 0.12 ± 0.01 mg BChl *c* (mg protein)$^{-1}$ vs. 0.15 ± 0.01 mg BChl *c* (mg protein)$^{-1}$. In addition, the *in vivo* absorbance peak for BChl *c* was 744–745 nm in strains Ω::RLP and Ω::SDR compared with 750 nm for WT2321, a 5–6 nm blue shift. The *in vivo* absorption maximum at 459 nm for the major carotenoid, chlorobactene, was not shifted. The blue shift was lost when BChl *c* was extracted into methanol. This observation suggested that the *in vivo* blue shift was not because of a structural property of BChl *c* in strains Ω::RLP and Ω::SDR, but rather reflected a difference in the degree of aggregation of BChl *c* compared with WT2321. A similar effect was seen in BChl *e* containing chlorosomes of another green sulfur bacterium, *Chlorobium phaeobacteroides*, which displayed a 10-nm blue shift when carotenoid biosynthesis was inhibited (37). No growth conditions were found to alleviate these effects in either strain.

Strain Ω::RLP exhibited a 3- to 4-fold defect in photoautotrophic growth rate compared with wild type in experimental cultures inoculated with midlogarithmic phase cultures (Table 1). Even with this growth rate defect, growth yield was not severely affected (data not shown). Acetate (6.5 mM) and, surprisingly, cysteine (0.5 mM) cured the growth defect. Serine (0.5 mM) did not cure the Ω::RLP growth defect, nor did pyruvate (5 mM) (data not shown). Photoautotrophic doubling times for wild type were 2.7 h compared with 3.8 h for strain Ω::RLP when stationary phase inocula were used, only a 1.4-fold effect. Thus, for unknown reasons, using stationary phase inocula greatly abrogated the observed photoautotrophic growth defect. Growth of strain Ω::SDR was the same as wild type under conditions where strain Ω::RLP growth was affected. Thus, the autotrophic growth defect in strain Ω::RLP was solely a consequence of the lack of the *C. tepidum* RLP.

Whole cell carbon fixation rates were determined in strain Ω::RLP and WT2321 (Table 1). Strain Ω::RLP exhibited a 2.9-fold lower photoautotrophic CO$_2$ fixation rate and a 1.6-fold lower photoheterotrophic CO$_2$ fixation rate when compared with WT2321. These defects were similar in magnitude to those seen for the photoautotrophic and photoheterotrophic growth rates (Table 1). Thus, decreased CO$_2$ assimilation capacity correlated with a decreased growth rate even under photoheterotrophic conditions.

Microscopic examination of cultures indicated that strain Ω::RLP accumulated more elemental sulfur globules than wild type. Normalization to the biomass of the cultures indicated that strain Ω::RLP had 2 × 10^7 sulfur globules (mg protein)$^{-1}$, whereas WT2321 had 5 × 10^6 sulfur globules (mg protein)$^{-1}$, a 4-fold difference. Elemental sulfur is the product of sulfide oxidation during phototrophic growth and is normally further oxidized to sulfate during later stages of growth, when sulfide and thiosulfate have been exhausted (4). Quantitation of elemental sulfur in cultures by extraction and UV spectroscopy confirmed the microscopy results (Fig. 4). Furthermore, cysteine (0.5 mM) was able to rescue the strain Ω::RLP phenotype, whereas serine (0.5 mM) did not (Fig. 4). Cysteine and serine did not appear to have any appreciable effect on elemental sulfur accumulation in WT2321 (data not shown). The level of *O*-acetylserine sulfhydrylase, the enzyme catalyzing the final step of cysteine biosynthesis from serine (27), was found to be similar in crude extracts of strain Ω::RLP and WT2321; 4.2 nmol min^{-1} (mg protein)$^{-1}$ vs. 3.4 nmol min^{-1} (mg protein)$^{-1}$, respectively. This result suggested that strain Ω::RLP is not merely a cysteine auxotroph and that cysteine may be having an indirect effect in curing the observed phenotypes.

When extracts of strain Ω::RLP and WT2321 were compared by SDS/PAGE, it was clear that strain Ω::RLP hyperaccumulated a polypeptide or polypeptides of ≈25 kDa in size compared with the wild type (Fig. 5). In contrast to the growth and sulfur oxidation phenotypes, the accumulation of this band was not affected by the presence of cysteine in the medium. Two N-terminal sequences were obtained from the hyperexpressed
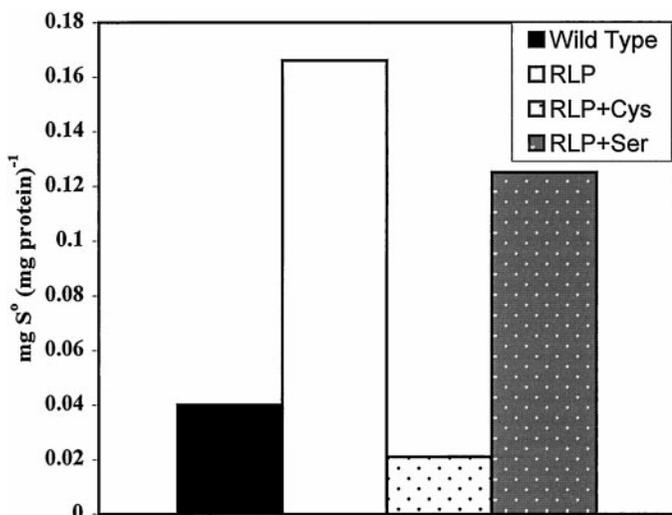
Fig. 4. Elemental sulfur levels in early stationary phase ($\approx$220 μg protein ml^{-1}) autotrophic cultures of WT2321 and strain Ω:: RLP. Media additions: Cys, 0.5 mM cysteine; Ser, 0.5 mM serine.

Fig. 6. Superoxide dismutase activity in crude extracts of WT2321 (wild type), strain Ω:: RLP (RLP) and strain Ω::SDR (SDR). Data represent the mean $\pm$ standard deviation of three independent cultures for each strain. One unit of specific activity corresponds to the amount of protein required to inhibit 50% of the rate of cytochrome c reduction by xanthine oxidase in an extract free standard assay (26).

band. The stronger sequence, N-SVLVGRPAPDFNA-C, uniquely identified a single ORF in the *C. tepidum* genomic sequence encoding a 21.8-kDa predicted protein belonging to the thiol-specific antioxidant/alkylhydroperoxide reductase (Tsa/AhpC) superfamily of oxidative stress proteins (38). The weaker sequence, N-AYQQPALPYA-C, uniquely identified an ORF encoding a 22.1-kDa predicted protein homologous to iron superoxide dismutases (Fe-SODs) (39). SOD activity was assayed in the wild type, Ω::RLP, and Ω::SDR strains. Consistent with the observed protein accumulation, strain Ω::RLP displayed 3- to 4-fold elevated SOD activity compared with WT2321 or strain Ω::SDR (Fig. 6).

Discussion

It is apparent that a RLP is synthesized by green sulfur bacteria. The *Chlorobium* RLPs are related to other bacterial and archaeal RLP sequences and form a distinct branch when phylogenetic trees of RubisCO sequences were generated. All RLP sequences lacked conserved active site residues present in *bona fide* RLPs. The *Chlorobium* RLPs are extreme in this regard, lacking nearly half of the key active site residues. Perhaps not
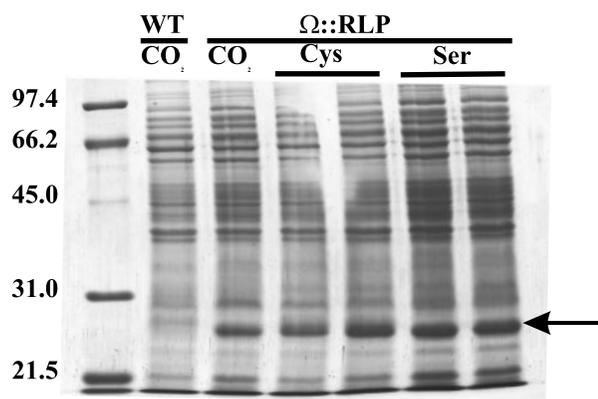

Fig. 5. SDS/PAGE analysis of 20 μg of cell extract protein from WT2321 (WT) or the Ω:: RLP mutant strain (Ω:: RLP). CO$_2$, photoautotrophic growth; Cys, photoautotrophic + 0.5 mM cysteine; Ser, photoautotrophic + 0.5 mM serine. Each lane contains cell extract from independent cultures harvested after 16 h of growth.
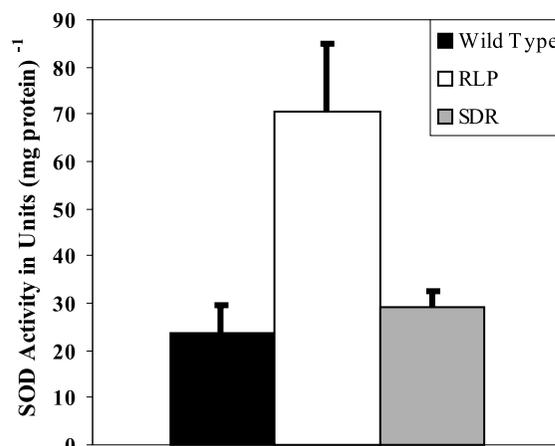
surprisingly, no significant RubisCO activity could be detected in *C. tepidum* extracts or with purified recombinant RLP.

The precise function of the *C. tepidum* RLP remains to be discovered. However, it is clear that the *C. tepidum* RLP influences the overall physiology of this organism as judged by the pleiotropic phenotype observed in strain Ω::RLP. We hypothesize that the observed decreases in photoautotrophic growth rates and carbon fixation rates are because of a defect in the oxidation of sulfur compounds, such as elemental sulfur or thiosulfate, which provide reducing power for carbon fixation after the exhaustion of sulfide. None of these phenotypes were observed in strain Ω::SDR, demonstrating that they result specifically from inactivation of the gene encoding the *C. tepidum* RLP. That the sulfur oxidation defect did not affect the growth yield indicated that strain Ω::RLP was not completely blocked in these processes but was simply less efficient than strain WT2321. More detailed studies of sulfur metabolism in strain Ω::RLP are underway to more precisely define the defect in sulfur metabolism caused by lack of the RLP. We hypothesize that the addition of acetate reduces the demand for CO$_2$ fixation, as reflected by lower whole cell CO$_2$ fixation rates (Table 1). This observation implies a lower demand for reducing equivalents derived from sulfur compounds and most likely explains why the addition of acetate physiologically complements the autotrophic growth phenotype of strain Ω::RLP. That acetate did not fully complement the growth defect may be reflective of a defect in antenna efficiency arising from the decreased levels and increased aggregation of Bchl c in strain Ω::RLP.

Whether the accumulation of oxidative stress proteins was because of defective sulfur metabolism in strain Ω::RLP or caused the defect is unclear. Overexpression of genes encoding oxidative stress proteins occurs in a *B. subtilis* mutant lacking the *ahpC* gene, encoding a subunit of the alkylhydroperoxide reductase, where SOD and other members of the peroxide regulon are compensatorily derepressed (40). This observation may suggest that the *C. tepidum* RLP is involved in an oxidative stress response. If that is the case, then alternative hypotheses can be proposed for the role of the *C. tepidum* RLP. First, the *C. tepidum* RLP may itself be an oxidative stress response protein and play a role in preventing the accumulation of molecules responsible for oxidative stress such as organic radicals or reactive oxygen species. If this were true, then the *C. tepidum*

Hanson and Tabita

RLP might specifically be positively regulated by oxidative stress conditions. Secondly, the *C. tepidum* RLP may not be directly involved in the oxidative stress response but may serve as a marker that the cell uses to monitor oxidative stress levels. In this case, we hypothesize that the activity or integrity of the *C. tepidum* RLP should be negatively affected by oxidative stress. Both hypotheses could account for the observed overexpression of Tsa/AhpC and Fe-SOD seen in strain Ω::RLP but do not directly account for the other phenotypes observed unless these characteristics are indicative of an oxidatively stressed state in *C. tepidum*.

An attractive hypothesis that potentially explains the oxidative stress and sulfur oxidation phenotypes seen in strain Ω::RLP is that the *C. tepidum* RLP is involved in synthesizing or recycling a small molecular weight thiol compound, possibly glutathione or a modified glutathione. This hypothesis may also explain why cysteine physiologically complements the growth and sulfur accumulation phenotypes. There is some precedence in purple sulfur bacteria that glutathione amide may be involved in the attack on periplasmic elemental sulfur as the first step in its oxidation to sulfate (41). The situation would be somewhat more complicated in *C. tepidum*, as elemental sulfur is deposited extracellularly, not periplasmically. A reduced level of such a compound in strain Ω::RLP could explain a reduced capacity for elemental sulfur oxidation and likely explain the aberrant expression of oxidative stress genes if this molecule is also used to monitor the oxidative stress status of the cell. This may explain why cysteine, as a generic low molecular weight thiol, is able to physiologically complement the growth and sulfur accumulation phenotypes. That cysteine does not restore wild-type regulation to the oxidative stress proteins suggests that cysteine is most likely not directly used to monitor the oxidative stress status of the cell in *C. tepidum*.

Irrespective of the specific physiological role of the *C. tepidum* RLP, it is clearly dispensable for growth. That eliminating synthesis of this protein in *C. tepidum* by gene disruption was not conditionally lethal under the conditions tested suggested that most point mutations would have a similarly benign effect. This observation leads to the hypothesis that RLPs might be good candidates for the evolutional precursors of extant *bona fide* RubisCOs found in plants, bacteria, and archaea (1). Thus, further study of RLPs might prove useful to probe a potential evolutional avenue toward the development of a functional RubisCO active site, while revealing much about what is required for enzyme specificity. At this time, it certainly cannot be ruled out that RLPs might represent intermediates in evolutional processes that lead away from *bona fide* RubisCO function, i.e., toward alternative activities. In any case, these interesting evolutional relatives of RubisCO might prove interesting to determine how diverse proteins might use carbamylation motifs for functions other than CO_2 fixation.

1. Tabita, F. R. (1999) *Photosynth. Res.* **60,** 1–28.
2. Cleland, W. W., Andrews, J. T., Gutteridge, S., Hartman, F. C. & Lorimer, G. H. (1998) *Chem. Rev.* **98,** 549–561.
3. Buchanan, B. B. & Arnon, D. I. (1990) *Photosynth. Res.* **24,** 47–53.
4. Brune, D. C. (1989) *Biochim. Biophys. Acta* **975,** 189–221.
5. Evans, M. C. W., Buchanan, B. B. & Arnon, D. I. (1966) *Proc. Natl. Acad. Sci. USA* **55,** 928–934.
6. Buchanan, B. B., Schürmann, P. & Shanmugan, K. T. (1972) *Biochim. Biophys. Acta* **283,** 136–145.
7. Buchanan, B. B. & Sirevag, R. (1976) *Arch. Microbiol.* **109,** 15–19.
8. Sirevag, R. (1974) *Arch. Microbiol.* **98,** 3–18.
9. Tabita, F. R., McFadden, B. A. & Pfennig, N. (1974) *Biochim. Biophys. Acta* **341,** 187–194.
10. Ivanovsky, R. N., Sintsov, N. V. & Kondratieva, E. N. (1980) *Arch. Microbiol.* **128,** 239–241.
11. Fuchs, G., Stupperich, E. & Jaenchen, R. (1980) *Arch. Microbiol.* **128,** 56–63.
12. Fuchs, G., Stupperich, E. & Eden, G. (1980) *Arch. Microbiol.* **128,** 64–71.
13. Andersson, I., Knight, S., Schneider, G., Lindqvist, Y., Branden, C.-I. & Lorimer, G. H. (1989) *Nature (London)* **337,** 229–234.
14. Chapman, M. S., Suh, S. W., Curmi, P. M., Cascio, D., Smith, W. W. & Eisenberg, D. S. (1988) *Science* **241,** 71–74.
15. Newman, J. & Gutteridge, S. (1993) *J. Biol. Chem.* **268,** 25876–25886.
16. Altamirano, M. M., Blackburn, J. M., Aguayo, C. & Fersht, A. R. (2000) *Nature (London)* **403,** 617–622.
17. Mukhopadhyay, B., Johnson, E. F. & Ascano, M. J. (1999) *Appl. Environ. Microbiol.* **65,** 301–306.
18. Wahlund, T. M. & Madigan, M. T. (1993) *J. Bacteriol.* **175,** 474–478.
19. Wahlund, T. M. & Madigan, M. T. (1995) *J. Bacteriol.* **177,** 2583–2588.
20. Wahlund, T. M., Woese, C. R., Castenholz, R. W. & Madigan, M. T. (1991) *Arch. Microbiol.* **156,** 81–90.
21. Ausubel, F. M., Brent, R., Kingston, R. E., Moore, D. D., Seidman, J. G., Smith, J. A. & Struhl, K. (1987) *Current Protocols in Molecular Biology* (Green & Wiley, New York).
22. Prentki, P. & Krisch, H. (1984) *Gene* **29,** 303–313.
23. Chung, S., Shen, G., Ormerod, J. & Bryant, D. A. (1998) *FEMS Microbiol. Lett.* **164,** 353–361.
24. Grimberg, J., Maguire, S. & Belluscio, L. (1989) *Nucleic Acids Res.* **17,** 8893.
25. Dubbs, J. M., Bird, T. H., Bauer, C. E. & Tabita, F. R. (2000) *J. Biol. Chem.* **275,** 19224–19230.
26. Crapo, J. D., McCord, J. M. & Fridovich, I. (1978) *Methods Enzymol.* **53,** 382–393.
27. Droux, M., Martin, J., Sajus, P. & Douce, R. (1992) *Arch. Biochem. Biophys.* **295,** 379–390.
28. Altschul, S. F., Gish, W., Miller, W., Myers, E. E. & Lipman, D. J. (1990) *J. Mol. Biol.* **215,** 403–410.
29. Grundy, F. J. & Henkin, T. M. (1998) *Mol. Microbiol.* **30,** 737–749.
30. Miziorko, H. M. & Sealy, R. C. (1980) *Biochemistry* **19,** 1167–1171.
31. Watson, G. M. F., Yu, J.-P. & Tabita, F. R. (1999) *J. Bacteriol.* **181,** 1569–1575.
32. Nagao, T., Mitamura, T., Wang, X. H., Negoro, S., Yomo, T., Urabe, I. & Okada, H. (1992) *J. Bacteriol.* **174,** 5013–5020.
33. Ghosh, D., Weeks, C. M., Grochulski, P., Duax, W. L., Erman, M., Rimsay, R. L. & Orr, J. C. (1991) *Proc. Natl. Acad. Sci. USA* **88,** 10064–10068.
34. Chung, S. & Bryant, D. A. (1996) *Arch. Microbiol.* **166,** 234–244.
35. Xie, D. L., Lill, H., Hauska, G., Maeda, M., Futai, M. & Nelson, N. (1993) *Biochim. Biophys. Acta* **1172,** 267–273.
36. Chung, S. & Bryant, D. A. (1996) *Photosynth. Res.* **50,** 41–59.
37. Arellano, J. B., Psencik, J., Borrego, C. M., Ma, Y. Z., Guyoneaud, R., Garcia-Gil, J. & Gillbro, T. (2000) *Photochem. Photobiol.* **71,** 715–723.
38. Chae, H. Z., Robison, K., Poole, L. B., Church, G., Storz, G. & Rhee, S. G. (1994) *Proc. Natl. Acad. Sci. USA* **91,** 7017–7021.
39. Liu, Y., Zhou, R. & Zhao, J. (2000) *Biochim. Biophys. Acta* **1491,** 248–252.
40. Bsat, N., Chen, L. & Helmann, J. D. (1996) *J. Bacteriol.* **178,** 6579–6586.
41. Bartsch, R. G., Newton, G. L., Sherril, C. & Fahey, R. C. (1996) *J. Bacteriol.* **178,** 4742–4746.